



Stabilizing a post-landslide loess slope with anti-slide piles in Yan'an, China

Hao Li¹ · Qin-wen Du¹

Received: 4 August 2020 / Accepted: 14 October 2021 / Published online: 31 October 2021
© The Author(s), under exclusive licence to Springer-Verlag GmbH Germany, part of Springer Nature 2021

Abstract

Anti-slide piles are economical and effective slope-retaining structures that are widely used in highway subgrade protection, and the mechanism of these piles has been attracting increasing attention. In this study, a cutting loess slope in Shaanxi Province, China, was excavated during the construction of a highway, and a row of anti-slide piles was used in the field to stabilize the slope. The results of in situ surveys and drilling indicated that a landslide had previously occurred. To ensure the safety of the slope, detailed monitoring measures were applied. Soil boreholes and pile monitoring holes were drilled to investigate the horizontal displacement. The pile length was 40 m with a cross section of 2 m × 3 m and a pile spacing of 6 m. To explore the interaction between high slopes and long anti-slide piles, a three-dimensional numerical model was established. Thereafter, the stress and deformation characteristics of a single pile were studied, and factors such as the pile length, embedment ratio, pile spacing, and cross section were considered. A comparison of the simulation and measurement results demonstrated that increasing the pile length may cause a shallow landslide, leading to a lower safety factor of the slope. It was found that $s=4b$ can be thought of as the most cost-effective arrangement and the soil arching effect in the vertical direction of 8–20 m is stronger; the earth pressure behind the pile will decrease due to the friction between the bedrock and soil near the sliding surface. It was also found that rectangular piles are more suitable for stabilizing high slopes. This study provides optimization choices for the slope and has reference value in the application of stabilizing piles.

Keywords Anti-slide pile · Stability · Strength reduction · Deformation · Stress

Introduction

The anti-slide pile is a kind of typical horizontally loaded pile that provides an effective measure for stabilizing slopes. As passive piles, the stress acting on anti-slide piles is caused by the movement of the soil around the pile (Guo 2015). The working mechanism of the anti-slide piles is to transfer the driving force of a landslide to the bedrock ground below the sliding surface so that the slope can be reinforced. (Li et al. 2016).

Many researchers have conducted theoretical studies on the stability of slopes reinforced with piles. The

limit-equilibrium method (LEM) and limit analysis method (LAM) are always adopted for analysis. In the aspects of LEM, a simplified approach based on an uncoupled formulation was presented, in which the pile response and slope stability were considered separately (Lee et al. 1995). An approach was developed by extending the simplified Bishop slice method to analyze the stability of a strain-softening slope reinforced with stabilizing piles, revealing that the stability was dependent not only on the strength parameters but also on the stress–strain relationship of soil (Zhang and Wang 2010). In addition, a new LEM was established for analyzing the stability of slopes reinforced with micropiles (Deng et al. 2017). In terms of LAM, the plastic state theory was developed and employed to assess the pressure acting on the piles regardless of the state of equilibrium of the slope (Ito and Matsui 1975). This theory was originally used for rigid piles and was not suitable in most cases. However, it was extended for use in flexible piles under the assumption of small deformation (Ito et al. 1981). An approach accounting for changes of critical surface due to the presence of the

✉ Qin-wen Du
duqinwen@chd.edu.cn

Hao Li
2018021005@chd.edu.cn

¹ School of Highway, Chang'an University, The Middle of South Second Ring Road, Xi'an, Shaanxi Province, People's Republic of China

piles was subsequently developed (Hassiotis et al. 1997). Based on the upper bound of limit analysis, the plane-strain analysis of the slopes reinforced with a row of piles was extended to the 3D case (Gao et al. 2015) and unsaturated soils were studied (Yuan and Du 2018; Deng and Yang 2019).

In the aspect of numerical research, most studies have explored the interaction between piles and slopes through multiple models, and proved the superiority of numerical simulation (Won et al. 2005; Yuan et al. 2021; He et al. 2015). With the help of numerical analysis, some researchers have also studied the failure mechanism of the slope and the behavior of the fracture surface (Michalowski and Drescher 2009; Lim et al. 2016; Yang and Xu 2017; Li et al. 2021). Sensitive analysis of the parameters appearing in the pile–soil system were discussed in detail, such as pile spacing, interface roughness, relative displacement between the soil and pile, bending stiffness (Cai and Ugai 2000; Rifat Kahyaoglu et al. 2009), soil property, pile position, surcharge distance, etc. (Sharafi and Sojoudi 2016). Moreover, the behavior of a strip footing supported on a row of piles and sheet pile-stabilized sandy slope was studied (El Sawwaf 2005). These studies further revealed the failure behaviors of slopes and were meaningful for theoretical research.

Anti-slide piles are widely used around the world. Table 1 summarizes numerous applications of piles for stabilizing slopes or other structures. It can be observed that most lengths of anti-slide piles appearing in the literature ranged from 20 to 30 m, which accounted for 44.5% (Fig. 1), followed by pile lengths of 20–30 m and 30–36 m, which both accounted for 22.2%. Piles that were less than 10 m were rarely used, which only accounted for 11.1%, indicating that anti-slide piles are more common in deep landslide treatment.

This study aims to evaluate the safety of a slope stabilized with long anti-slide piles. The movements of soil and anti-slide piles were observed through field monitoring methods,

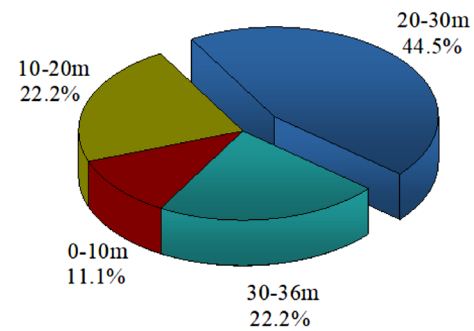


Fig. 1 Proportion of anti-slide pile length

and a three-dimensional finite element numerical model was established to study the pile–soil interaction of a high-loess slope. It not only provides optimization choices for this slope, but also has reference value in the wider application of stabilizing piles.

Project overview

General description

The cutting slope of the highway project, which is located in the west of Yan'an city, Shaanxi Province, China, where the terrain is complex and belongs to the typical loess area, a landslide disaster occurred in history. The height of the slope is 108 m, with two slope angles of 45° and 63°, as well as a length of 175 m in the slope direction.

According to the drilling results in the field, the formation layer at the slope can be divided into three types. The first type is the sliding soil that exists on the upper part of the slope and is mainly composed of powdered clay mixed with some gravels. The second type is the bed soil underneath the topsoil, which is composed of Q2 loess and some red clay

Table 1 Statistical samples of anti-slide pile lengths appearing in the literature

No.	Literature	Location	Pile length (m)
1	(Xu and Niu 2014)	Zhejiang, China	20
2	(Ashour and Ardalán 2012)	Hildenborough, Kent, UK	10
3	(Karim 2013)	Sydney, Australia	22.2
4	Onyango and Zhang (2019)	Guizhou, China	22
5	(Zheng et al. 2020)	Guizhou, China	23–32
6	(Zhang et al. 2020)	Chengdu, China	19 and 33
7	(Liu et al. 2020)	Three Gorges Reservoir, China	22
8	(Li et al. 2017)	Yichang, China	36
9	(Zhao et al. 2019)	Yunan, China	15–25 and 20–30
10	(Ersoy et al. 2020)	Ulbey, NE Turkey	25
11	(Xie et al. 2020)	Guizhou, China	9–16
12	(Premalatha et al. 2017)	Chennai port, India	30

(N2). The deposits present a hard state and calcium nodules are occasionally visible. The third type of layer consists of strongly and moderately weathered sandstone buried to a considerable depth. Because of a wide range of strata here, there are significant differences in engineering geological properties. It is assumed that the contact surface between two different soil layers could cause a potential landslide, especially the surface between the soil and bedrock. The strength and modulus of overlying soil above the bedrock are far less than those of underlying strongly and moderately weathered sandstone. Therefore, this surface becomes weaker with saturation under surface water infiltration, and sliding could happen along this weakness plane.

To stabilize the slope, some measures had been conducted before the highway construction. For example, the slope was cut to reduce its weight with the slope rate of 1:1.0 and 1:0.5, and the heights of the platform were 8 m and 6 m, respectively. In addition, a large area was also created to prevent the collapsed soil from falling into the highway. The second measure was the use of anti-slide piles. A row of anti-slide piles was set up on the third platform, each with a length of 40 m. The spacing of adjacent piles was 6 m with a cross section of $2\text{ m} \times 3\text{ m}^2$. Further measures including planting grass and setting up arched skeletons on slopes were also carried out. Figure 2 shows the overall view of this slope.

Monitoring scheme

Due to the large height of the slope and the huge stress acting on the anti-slide piles, the horizontal displacement of the soil and pile must be monitored to ensure the safety of the slope. The monitoring results can reflect whether the slope is in a safe state, and can be used to warn of possible disasters in a timely manner.



Fig. 2 Overview of slope

To investigate the displacement of the pile–slope system, a number of inclinometers were installed. To observe the displacement of the soil, two boreholes were drilled in the field with a depth of 50 m. The inclinometers were attached to PVC tube and buried into the boreholes, and the hole was backfilled with sand and grouted finally.

The sensors for measuring anti-slide pile displacement were relatively smaller and could be inserted into PVC tubes. The anti-slide pile was pre-buried with acoustic testing pipes during construction, which can be used directly as a channel to monitor pile deflection, eliminating the process to drill holes in the pile. Figure 3 shows the installation method of these monitoring sensors. Two boreholes for monitoring soil displacement were set on the fourth platform, symmetrically located on both sides of the pile, and anti-slide piles were set on the third platform. To facilitate discussion here, the soil boreholes are numbered BH01 and BH02, and the pile hole is numbered BH03. Table 2 shows the position of the inclinometers in the boreholes.

Measured results and analysis

The displacement monitoring activities were carried out a few months after the slope construction was completed. Therefore, only the relative displacement within the monitoring period could be obtained, and the displacement occurring during construction could not be observed.

The horizontal displacements of the two boreholes BH01 and BH02 are shown in Fig. 4a, b. The monitoring began in December 2016 and lasted until August 2017, when the deformation of the soil and piles had stabilized. BH01 and BH02 show similar trend of displacement, the displacement at the bottom is smaller, and the maximum displacement appears at the top of the hole, with a maximum displacement of 31.6 and 37 mm, respectively. The rate of increase in the horizontal displacement of both BH01 and BH02 slows down in May 2017. This suggested that the soil became stable and large displacements were unlikely to occur after that date. However, during this period, the relative displacement of the inclinometer between 23 and 28 m was larger. From the results of the in situ survey, it was the soil–rock interface, which is prone to cause the soil sliding along the rock below. Similar to soil displacement, the pile head showed maximum displacement, at 32 mm, the displacement below the sliding surface is relatively small, showing the cantilever beam's characterization, and the pile head displacement became stable after April 2017, as Fig. 4c shows, and the soil arching between the piles was produced.

Shear strength reduction method

With the widespread use of computers, finite element method (FEM) analysis of slope stability has advanced

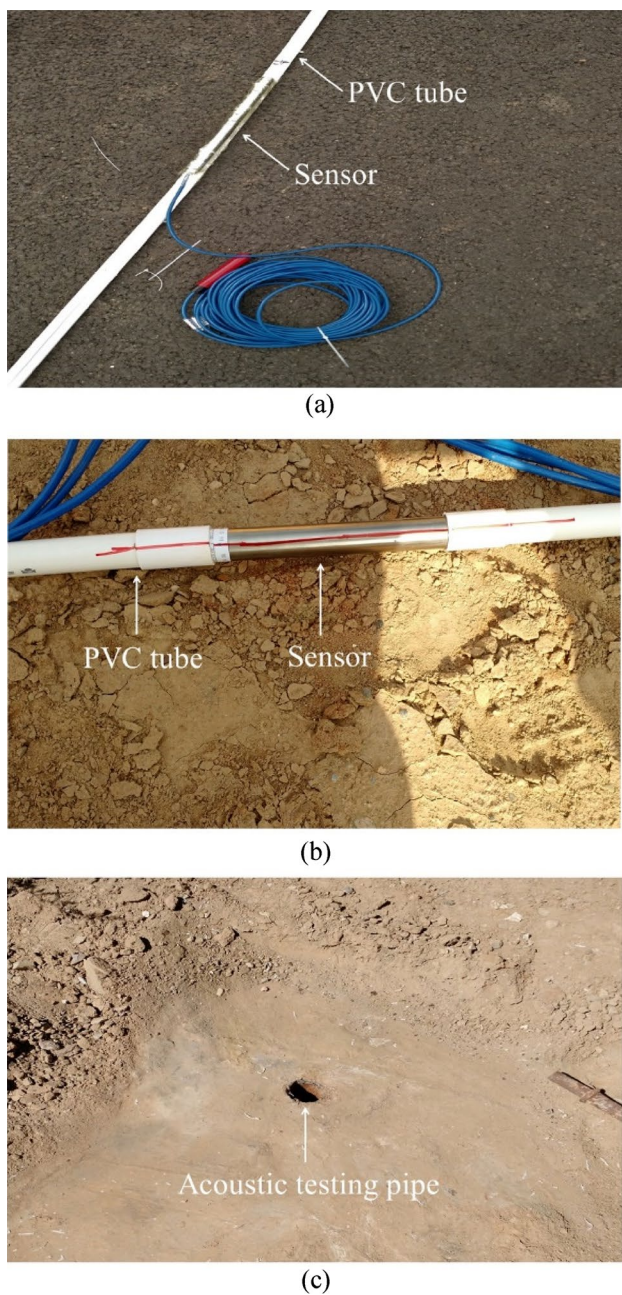


Fig. 3 **a** Installation of sensors in soil. **b** Installation of sensors in pile. **c** Reserved acoustic testing pipe on pile

Table 2 Sensor position

Bore hole No.	Position (m)
01	3-8-13-18-23-28-38-48
02	3-8-13-18-23-28-38-48
03	2-5-8-13-18-23-31-40

significantly in recent years. In this paper, the slope model is established through the finite element code Abaqus and the shear strength reduction method (SSR) is used.

Shear strength parameters have a great influence on the safety factor F_s of the slope. In this work, the parameters of the original soil and rock were obtained from the field investigation and associated laboratory and field tests. The values are provided in Table 3. As shown in Fig. 5, the soil in region I is mainly Q2 loess, region II is red clay, regions III and IV is sandstone, and region V is composed of Q2 loess with some gravels.

SSR can be used to analyze the stability of the slope, while FEM can obtain a safety factor directly. The strength reduction factor is expressed by F_r , and the shear strength parameters after reduction can be expressed as:

$$c_m = \frac{c}{F_r}, \quad (1)$$

$$\varphi_m = \arctan\left(\frac{\tan\varphi}{F_r}\right), \quad (2)$$

where c , φ represent the actual cohesion and friction angle of soil, and c_m and φ_m are the cohesion and friction angle after reduction. During calculation, the strength reduction factor F_r gradually increases, the reduction factor F_r is the safety factor F_s of the slope under the critical failure status ($F_r = F_s$), and the sliding surface can be obtained.

Model description

A three-dimensional numerical model was built to analyze the slope stability and the interaction between the pile and soil through the application of the finite element code Abaqus. As mentioned above, the slope soils consisting of loess, red clay and bedrock were all modeled as linear elastic perfectly plastic materials obeying a Mohr–Coulomb failure criterion, and stabilizing piles were modeled as linear elastic materials. The height of the slope was 108 m, with a length of 175 m, and pile length of 40 m. Because the numerical model represents only a section of the in situ slope, the direction of U3 for the front and back boundaries was constrained ($Z=0$), the location of the right and left end boundaries was far enough to allow the slide surface to fully develop, the horizontal direction (U1) of the right and left boundaries was restrained ($X=0$) and displacement along the bottom boundary was fixed horizontally and vertically ($X=Y=Z=0$). To simulate the pile embedded in the rock, the bottom of the pile was fixed ($X=Y=Z=0$), the initial stress equilibrium was performed to balance the internal and external and internal force, and thus the displacement due to the initial stress was eliminated. To reduce calculation time, only a symmetrical model was considered in this paper, the thickness of the model is 3 m, which equaled half the distance

Fig. 4 **a** Soil horizontal displacement in BH01. **b** Soil horizontal displacement in BH02. **c** Pile horizontal displacement

of adjacent piles and the width of the pile is 1 m, as shown in Fig. 6.

The interaction type between the pile and soil was arranged as a master–slave surface contact. The contact property of tangential behavior was “Penalty”, and the normal behavior was “Hard” contact. The element type was C3D8, and the mesh of the model is shown in the Fig. 7. The field variable FV, which represented the safety factor F_s of the slope, was varied from 0.5 to 2, with an increment of 0.25.

Displacement obtained by FEM

Figure 8 shows a comparison of the simulated soil displacement and measured evidence. The measured and simulated displacements exhibit the same trend, but the simulated displacement was greater. It can be interpreted that the simulated slope was in a critical state when the calculation was terminated and the soil displacement was the largest. As depicted in Fig. 4, soil displacement continued to increase, illustrating this slope far from reaching the critical state. Secondly, in situ monitoring started a period of time after the slope construction was completed, resulting in the measured displacement being less than the simulated displacement.

Figure 9 depicts that the simulated pile displacement and the measured value are in agreement when the depth is below 13 m, but the pile head displacements are largely different. The simulated pile head displacement is about 48 mm and the measured value is 32 mm. It can be interpreted that the soil in front of the pile has not reached the passive limit state so it can provide resistance; additionally, researches (Zhao et al 2019; Kourkoulis et al 2011) have found that embedment ratio, which is the pile segment embedded in the bedrock to that embedded in the sliding mass, had an influence on the deformation characteristics of the pile. The following section discusses the role of embedment ratio.

Due to the construction of the expressway, the geometric shape of the slope changed, resulting in varying the position of the most dangerous sliding surface of the slope. The simulated results show that the safety factor of the slope is 1.232, and the sliding surface corresponding to the safety factor stems from the fifth platform to the top of the slope, as shown in Fig. 10.

Discussion

Effect of pile length

Excessive length of anti-sliding piles will lead to increased deformation, higher costs, and will negatively affect

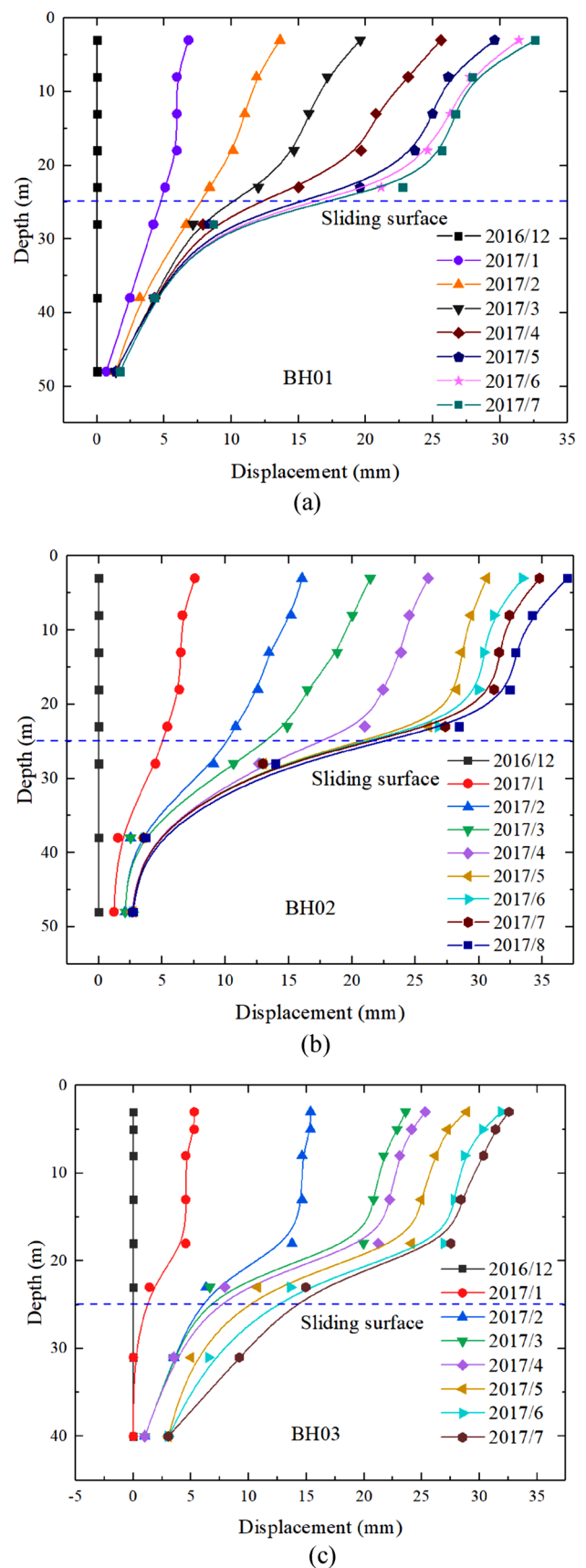


Table 3 Parameters of each soil layer

Region	Unit weight (kN/m ³)	Elastic modulus (MPa)	Cohesion (kPa)	Internal friction angle (°)	Poisson's ratio
I	20	10	25	35	0.4
II	20.5	25	150	23	0.3
III	20.5	120	90	25	0.2
IV	25	1500	400	28	0.2
V	19.5	18	36	31	0.4
Pile	25.0	3×10^4	–	–	0.2

Fig. 5 Slope model and soil layer distribution

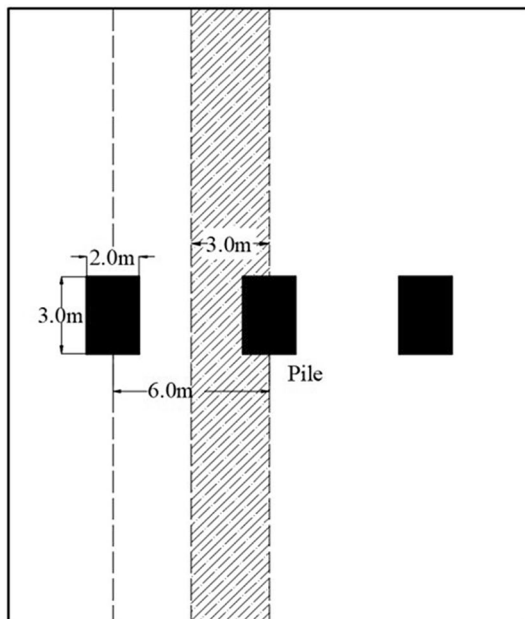
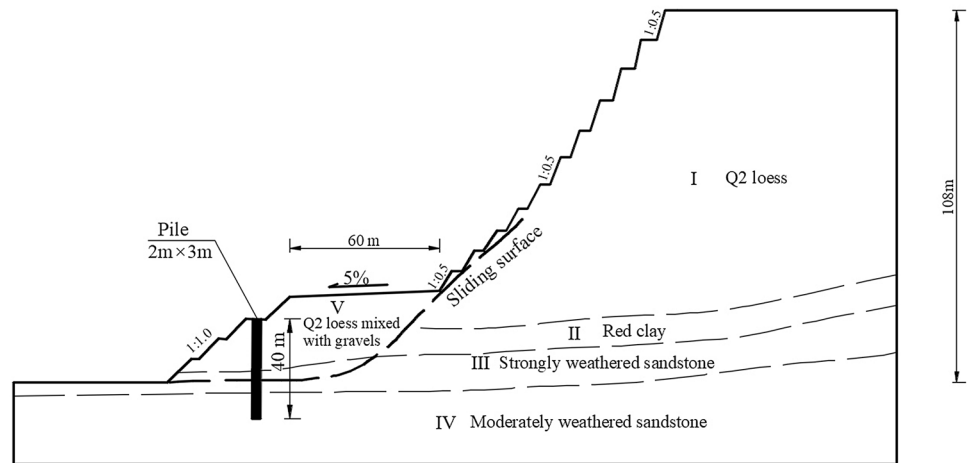


Fig. 6 Symmetrical analysis of piles and pile spacing

construction. However, insufficient length of piles will cause soil slide along the weakness surface. In general, the bottom of the anti-slide pile needs to be embedded in the

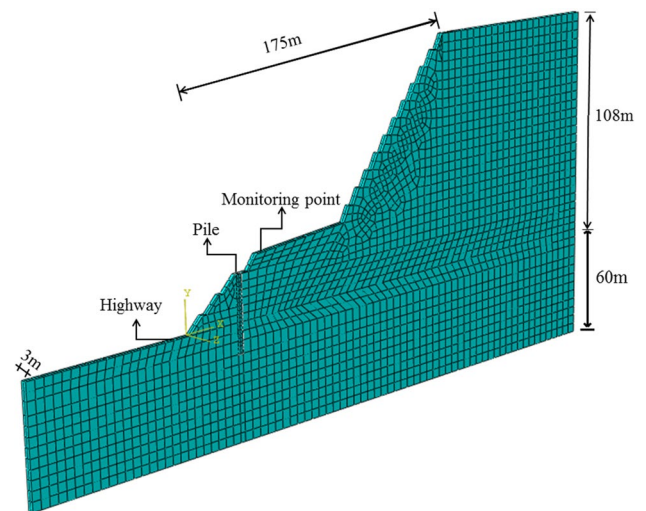


Fig. 7 Slope model overall mesh

rock to allow the pile to bear a greater sliding force. Proper pile length and embedment depth can make the design more economical and reasonable. The embedded ratios of the pile segment below the sliding surface to that embedded in the sliding mass usually range from 0.25 to 1.

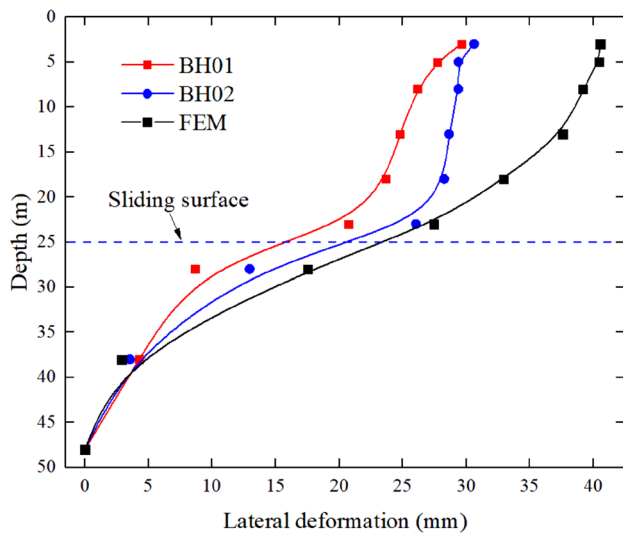


Fig. 8 Comparison between measured and simulated results of soil displacement

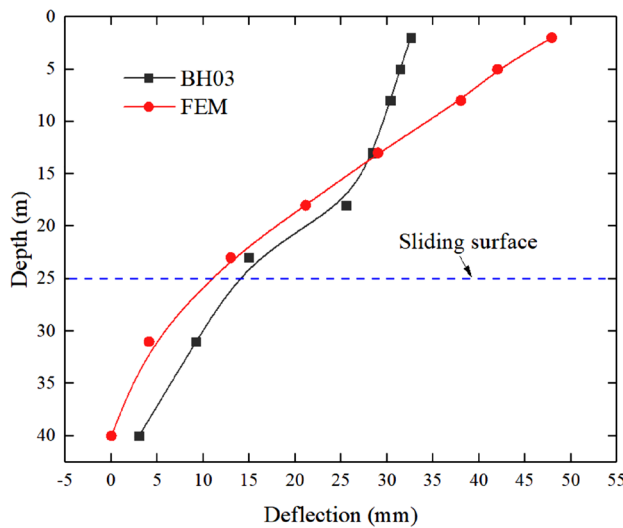


Fig. 9 Comparison between measured value and numerical result of pile deflection

Table 4 gives the specific pile length studied in the simulation. To study the global stability of the slope under varied pile lengths, seven numerical models with different pile lengths were established, and each model obtained a safety factor of the slope. In this study, different pile lengths mainly referred to the length below the sliding surface, which consisted of clay, strongly weathered sandstone and moderately weathered sandstone, with moderately weathered sandstone predominating with increased depth.

Figure 11 presents the pile head displacement and safety factors under different pile lengths. It can be found that the safety factor of the slope is less than 1.0 when the length is 37 m, which means that the slope is not under the safety

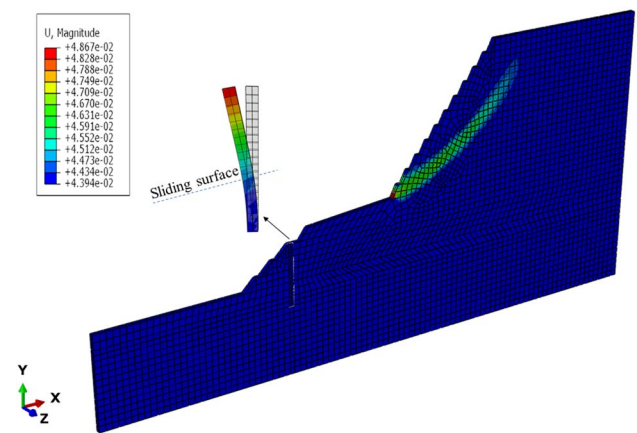


Fig. 10 Plastic zone and pile deflection of slope

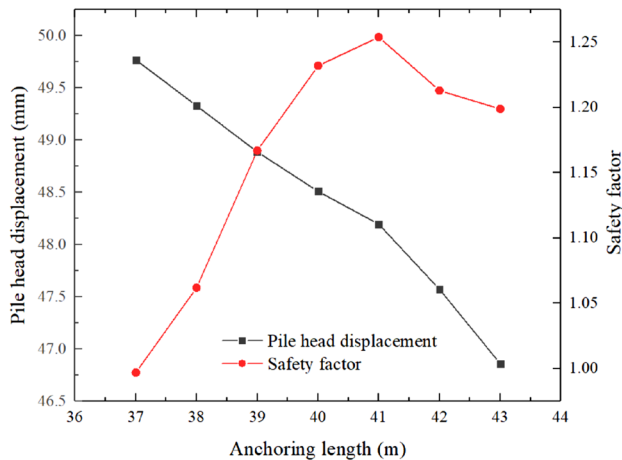
state. The reason may be that the depth embedded in the rock is not long enough so the displacement is too large. If the F_s of the slope is far less than 1.0, for example, $F_s = 0.7$, such a result is meaningless, because this slope has already slipped and cannot be reinforced. Actually, those slopes that need to be reinforced have an F_s close to 1.0. From Table 4, the slopes with pile lengths of 37 m and 38 m should further be reinforced. With the increase of pile length as well the depth embedded in the rock, the safety factor increases until the length is 41 m, then it decreases. In terms of safety factor, the most suitable pile length is 41 m with an embedded ratio of 0.64.

Figure 11 also illustrates the relationship between the pile head displacement and pile length. The pile head displacement gradually decreases as the pile length increases, indicating that increasing embedded length can reduce the pile head displacement. However, increasing the pile length means massive costs, harder construction conditions, and possible a lower safety factor; therefore, when designing anti-slide piles, it is necessary to ensure that the length of the pile meets the specifications, but is also economical.

Comparing Fig. 12a, b, it can be found that the plastic zone with a pile length of 43 m is closer to the slope surface than that of 40 m. In other words, a shallow landslide will occur more easily when the pile is 43 m, and the reduction in safety factor can be attributed to the occurrence of shallow landslides. However, Fig. 12 represents the assumed sliding surface calculated by FEM, which is related to the slope geometry. Therefore, the analysis of the safety factor is based on the assumed sliding surface and current slope geometry. In general, the location of the original sliding surface determines how the piles should be designed and constructed, and the piles for stabilizing this sliding surface keep the soil stable, almost impossible to flow between the piles. However, a new possible sliding surfaces may be generated in the

Table 4 Safety factor of slope with different pile lengths

Plan	Dimension (m)	Spacing (m)	Length (m)	Length below sliding surface (m)	Embedment ratio	F_s
1	2 m × 3 m	6	37	12	0.48	0.997
2			38	13	0.52	1.062
3			39	14	0.56	1.167
4			40	15	0.60	1.232
5			41	16	0.64	1.254
6			42	17	0.68	1.213
7			43	18	0.72	1.199

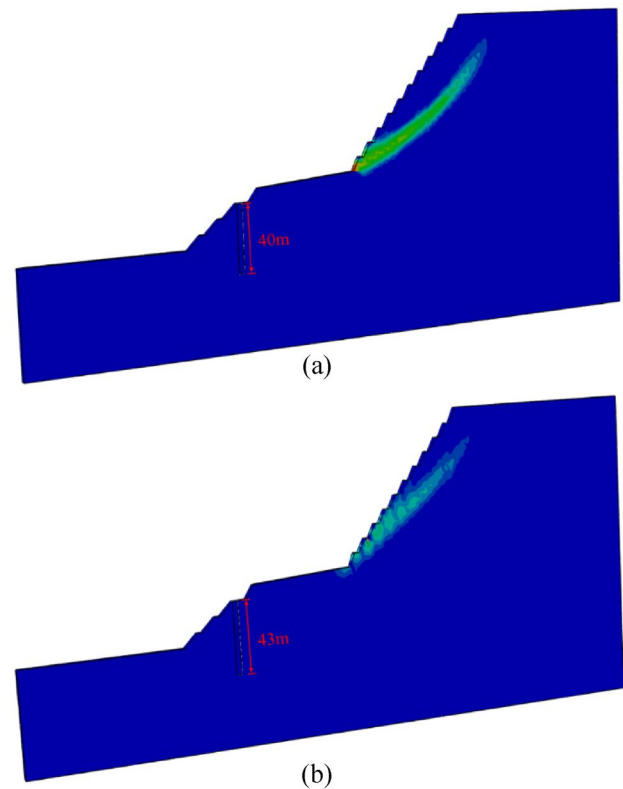
**Fig. 11** Safety factor and pile head displacement under different pile lengths

slope as the simulation shows. Therefore, it is necessary to consider the issue in field applications.

Effect of embedment ratio

To further study the effect of the pile length, the embedment ratio, namely the ratio of the pile segment embedded in the bedrock to that embedded in the sliding mass, is introduced. Table 4 reports the embedment ratios corresponding to different pile lengths.

The simulation results show that the safety factor F_s of the slope was less than 1.0 when the embedment ratio was 0.48, which implies that the embedment was not sufficient to provide adequate fixity conditions. Moreover, the value of F_s increased with the embedment ratio. But due to the effect of shallow landslide, F_s decreased when the ratio was between 0.68 and 0.72. As mentioned previously, the embedment ratio can affect the pile deformation pattern. When the embedment ratio is less than 0.7, a pile will exhibit characteristics similar to rigid piles, whereas when the ratio is greater than 1.2, a pile will exhibit flexibility, rather than rotation (Kourkoulis et al. 2011). The embedment ratio in

**Fig. 12** a Slope plastic zone when pile length is 40 m. b Slope plastic zone when pile length is 43 m

the field was about 0.6, leading to a different pile deflection pattern from that of the FEM.

Figure 9 illustrates that the actual pile exhibited a similar behavior of rigid inclination to some extent, while the FEM results indicated flexural deformation. Displacement monitoring was carried out a few months after the slope construction was completed. Therefore, the monitoring data can only indicate the relative displacement of the pile over this period and cannot reveal the deformation characteristics of the anti-slide pile from the beginning of construction. Thus, the time lapse and embedment ratio resulted in a difference between the measured pile deformation pattern and the FEM

results. From Fig. 11, it can be seen that the increase in the embedment ratio can effectively restrain the displacement of the pile head. To utilize the pile capacity and provide fixity conditions, a greater embedment ratio is required, but the increase of the embedment length will unavoidably be associated with increased installation costs. However, the economic impact is not the focus of the present study.

Effect of pile spacing

The principle that determines pile spacing is to prevent soil from sliding between piles, excessive pile spacing will cause soil sliding or pile damage due to excessive force, but the pile spacing is not as small as possible, a proper pile spacing can produce soil arching to transfer the soil pressure to the adjacent piles, where the two piles play the role of arching corner. Therefore, to stabilize the soil between the piles, it was suggested that the pile spacing should be 5–10 m (TB10025-2019) or 3–5 times the pile width (diameter).

During the transmission of earth pressure through the soil arching, it was determined that the earth pressure transmitted between the piles gradually decreased, and the earth pressure behind the piles increased significantly. Dong (2007) investigated the range of soil arching by measuring the soil pressure behind the piles, pointing that the sudden increase of soil pressure behind the piles can be a manifestation to determine the range of soil arching. From Fig. 19, it can be observed that the earth pressure displays a significant sudden change in the middle part of the sliding mass, in which the depth is 8–20 m, that is, the soil arching effect in this range is enhanced, however, due to the large lateral pile head displacement, the soil arching effect is relatively weak near the top of the pile, and the strength and range of the soil arching effect are nonlinearly distributed along the pile.

To determine the maximum pile spacing, a number of simulations with six different pile spacing, s , were performed and the response of the piles for $s = 2.5b, 3b, 3.5b, 4b, 4.5b$, and $5b$ were compared, where the pile width b is 2 m. The parameters of the piles and the safety factor of the slope obtained by FEM are listed in Table 5.

It was reported that the relationship between s/d and the slope safety factor was consistent with that of s/d and soil arching effect, and $s = 6d$ was the optimization (Zhang 2019), where d is the diameter of the round pile. For the rectangular-section pile in the present study, $s = 4b$ can be thought of as the most cost-effective arrangement, because it has the most significant spacing required to produce soil arching (in the range of 3–5 times the pile width) and the safety factor to ensure the slope’s stability, for $s = 4.5b$ and $s = 5b$, the safety factors are too low to ensure the slope’s stability.

Figure 13 shows a negative correlation between s/b and safety factors, but the increasing rate gets lower after $s/b > 4$.

Table 5 Safety factor of slope with different pile spacing

Plan	Width (m)	s/b	Pile head deformation (mm)	F_s
1	2	2.5	46.16	1.257
2		3	48.45	1.232
3		3.5	50.24	1.198
4		4	52.38	1.118
5		4.5	53.97	1.074
6		5	55.86	1.066

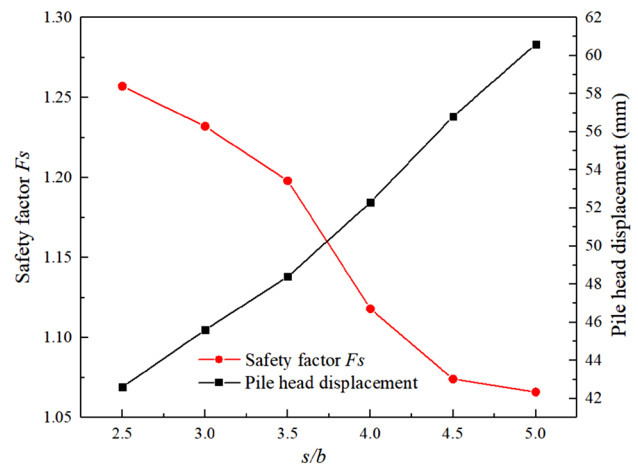


Fig. 13 Relationship between s/b and safety factor

That is, the soil arching effect becomes weaker, resulting in F_s decrease. The increase of s/b indicates that each pile is subjected to larger sliding force, leading to increased pile displacement, especially the pile head displacement, and the increase in the bending moment (Figs. 14 and 15). The pile head displacement increases from 46.16 to 55.86 mm. According to the Code for Design of Retaining Structures of Railway Earthworks (TB10025-2019), the allowed horizontal displacement for stabilizing piles is usually greater than that for other retaining structures, as suggested to control the pile head displacement according to different requirements. Generally, the pile head displacement is required to be less than 100 mm, which is considered in the present study to be compliant with the standard, regardless of the simulated conditions.

Stabilizing piles are usually regarded as cantilever beams, the segment above the sliding surface is subjected to landslide force and the segment below the sliding surface is subjected to soil resistance. The maximum bending moment is located at the soil–rock interface, with a depth of 26 m. As s/b increases, the soil arching effect will become weaker and disappear until s/b reaches a critical value.

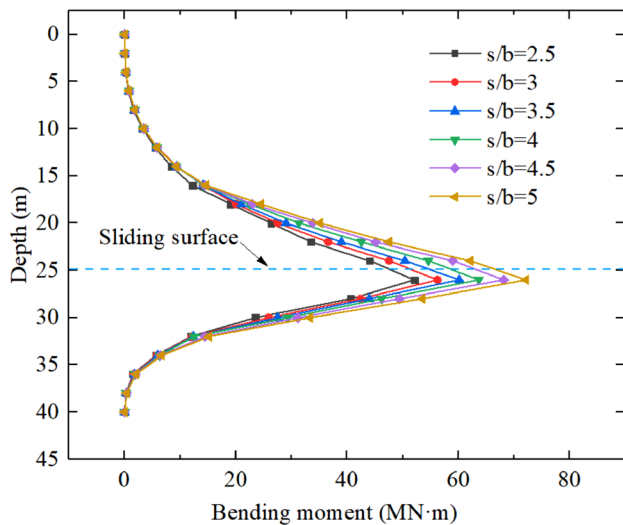


Fig. 14 Distribution of bending moment of pile under various s/b

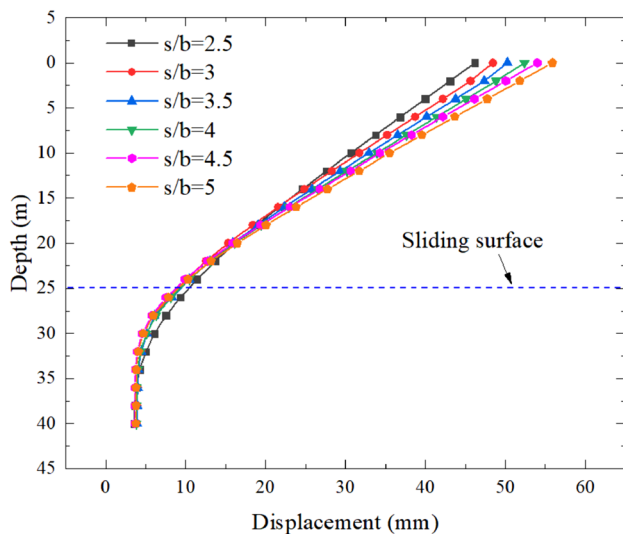


Fig. 15 Pile deflection under various s/b

Meanwhile, the earth pressure on the pile gradually increases and stabilizes. When the soil arching fails, the soil pressure on the pile decreases because the soil arching no longer delivers the sliding force to the piles. From Fig. 14, the bending moment on the pile gradually increases, indicating that the soil arch is effective in the range of $s = 5b$.

Effect of pile cross section

Under horizontal force, not only the soil in the width of the pile is compressed, but also the soil surrounding the pile is affected, showing a three-dimensional stress state.

In general, the spatial stress state is always converted into a plane problem. To consider the influence of the pile cross section, the pile width b or pile diameter d is converted into a rectangular pile with the width of B_p during calculation, which is equivalent to the actual width of the affected area. B_p is the calculated width of the pile.

For a rectangular section pile, its calculated width is denoted as:

$$B_p = b + 1. \tag{3}$$

For a round section pile, it is:

$$B_p = 0.9 \times (d + 1), \tag{4}$$

where b is the width of the rectangular pile and d is the diameter of the round piles. To make the calculated width the same in this paper, a rectangular pile with the width of 2 m and a round pile with a diameter of 2.4 m were studied, and other parameters of the piles were the same.

Figure 16 presents the plastic zone of the slope with a round pile, which is mostly the same as that in Fig. 10. The cross section of the pile has a great influence on the safety factor of the slope. The safety factor simulated with a round pile is 1.133, which is less than 1.232 for the rectangular pile. It can be interpreted that under the same calculated width B_p , the round pile's inertia quadrature and cross-sectional area are both smaller than that of the rectangular pile, which is not conducive to preventing the soil from moving.

Figure 17 shows the curve of the pile deflection under two cross sections. It can be observed that the cross section has nothing to do with the pile deflection pattern, the trends of the two curves are the same, and only the displacements are different, especially the pile head displacements. For the round pile, the pile head displacement is 50.6 mm, and for the rectangular pile, the pile head displacement is 48.5 mm.

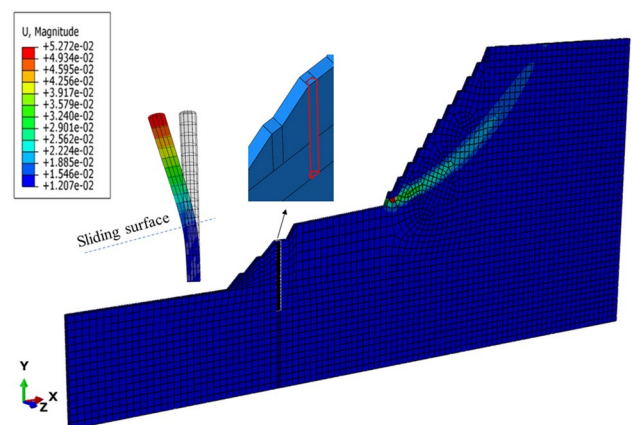


Fig. 16 Slope plastic zone and pile deflection under the condition of round piles

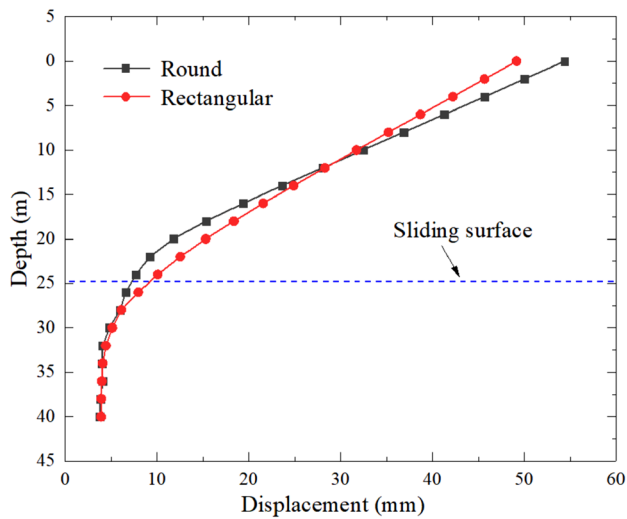


Fig. 17 Deflection of pile with different cross sections

Figure 18 presents a diagram of the pile bending moment. The trends of bending moment are in coherence, and the maximum bending moment appears near the sliding surface. However, the rectangular pile’s bending moment is 20% greater than that of the round pile. For the piles of the same calculated width, it is obvious that the rectangular pile not only restrains the pile head displacement, but also can bear greater bending moments. It can be attributed to the larger bending rigidity of the rectangular pile.

Figure 19 depicts the curve of earth pressure (CPRESS) behind the pile with different cross sections in the critical state. The curve obtained in this study is consistent with Yamin’s (2020) research. It can be found that the earth pressure behind the pile has an increasing trend along the pile,

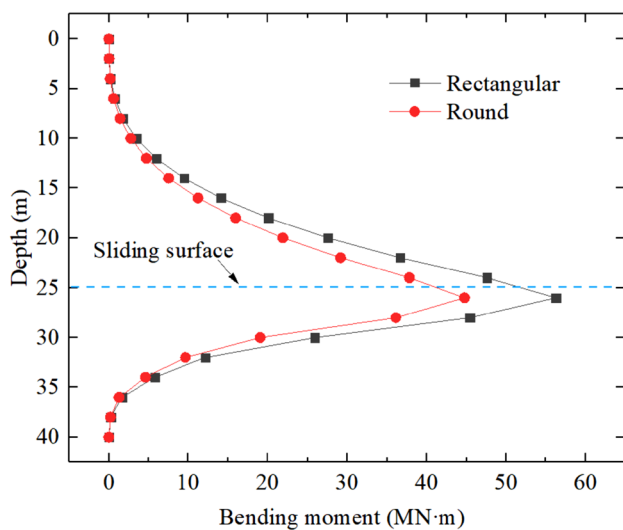


Fig. 18 Pile bending moments with different cross sections

but decreases near the sliding surface. The shape of the earth pressure curve of the round pile is like a parabola, but the rectangular pile is closer to a polyline. Generally, the distribution of earth pressure behind a structure is assumed as a triangle or rectangle-shaped, and sometimes trapezoid. However, the actual force acting on the pile is different. The sliding surface is the soil–rock interface; inevitably, there is sliding friction between the soil and rock, which offsets a portion of the earth pressure, leading to a decrease in the earth pressure near the sliding surface. Additionally, the displacement of the soil is large, while the pile displacement is small near the sliding surface according to the in situ monitoring results, the relative displacement between the pile and the soil releases part of the earth pressure, which may be the reason for the drop down in earth pressure as well.

Figure 20 shows a contour of the earth pressure acting on the pile. It reveals that the force acting on the pile is in coherence regardless of the cross section. At the sliding surface, the front of the pile is subjected to soil resistance, while below the sliding surface, the soil resistance behind the pile is greater, especially for rectangular piles.

Conclusion

In this research, soil and pile displacements were monitored, and a three-dimensional numerical slope model of a long anti-slide pile was established via Abaqus. The stability of the slope and the deformation and stress characteristics of the pile under different lengths, embedment ratios, pile spacing and cross sections were studied, and some conclusions can be made from the results as follows:

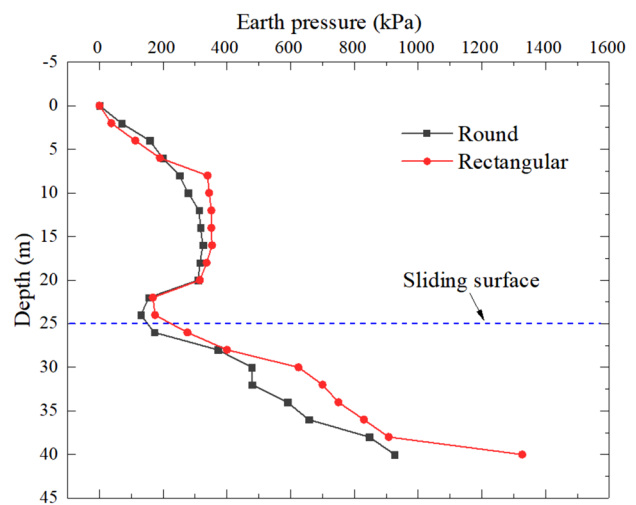


Fig. 19 Distribution of earth pressure behind the pile

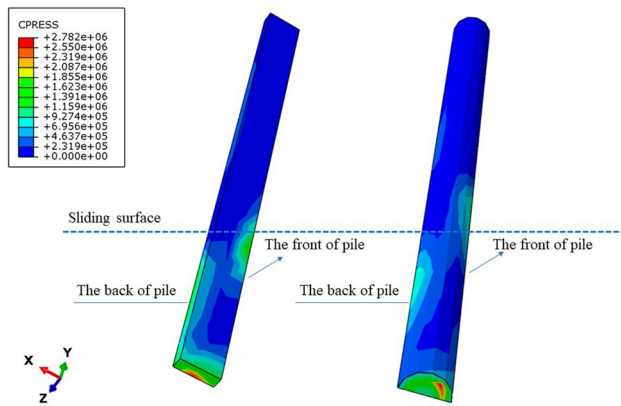


Fig. 20 Contour of pile contact pressure (earth pressure)

1. Increasing the pile length and embedment ratio can effectively reduce the pile head displacement. When the embedment ratio is greater than 0.68, the plastic zone gradually moves upward, which is more likely to cause shallow landslides, resulting in a lower global safety factor of the slope.
2. With the increase of the pile spacing, the safety factor decreases, but the displacement and bending moment of the pile gradually increase. The maximum bending moment appears near the sliding surface, because as the distance between the piles increases, each pile must bear a larger sliding force.
3. The soil arching effect in the vertical direction of 8–20 m is stronger, and the soil arching is effective between $s = 2b$ to $s = 5b$, but from the perspective of safety factor, $s = 4b$ is the most cost-effective pile spacing.
4. The cross section of the pile has an influence on the safety factor of the slope. Compared to a round pile, the pile head displacement of a rectangular pile is smaller while its bending moment is greater. This result illustrates that a rectangular pile is more suitable for high slopes.
5. The earth pressure behind the pile gradually increases along the pile, but decreases near the sliding surface. It can be interpreted that the friction between the soil and the sliding bed offsets a portion of the earth pressure.

As a study on the use of long anti-slide piles for high slopes, this paper presents optimizable choices and reveals the mechanisms of stress and deformation of long piles, providing a guiding role in the case study of slope reinforcement. However, due to field conditions, some data such as the earth pressure behind the pile were not monitored so that only analyzed by numerical calculation. In the future, a model test should be used to better simulate the behavior of long anti-slide piles and slope stability.

Acknowledgements The authors acknowledge the financial support provided by CCCC First Highway Consultants Co., Ltd, and would like to thank Professor Li for his help in the design of the field monitoring program, as well as the help of Li and Xia in the field tests.

Author contributions All authors listed on the manuscript contributed to the study and approved the current version of the manuscript.

Funding This project received financial support by CCCC First Highway Consultants Co., Ltd.

Availability of data and material Data and material in this study are available.

Code availability The code Abaqus in this study is available.

Declarations

Conflict of interest There are no conflicts of interest.

References

- Ashour M, Ardalan H (2012) Analysis of pile stabilized slopes based on soil-pile interaction. *Comput Geotech* 39:85–97. <https://doi.org/10.1016/j.compgeo.2011.09.001>
- Cai F, Ugai K (2000) Numerical analysis of the stability of a slope reinforced with piles. *Soils Found* 40(1):73–84. <https://doi.org/10.3208/sandf.40.73>
- China Railway Eryuan Engineering Group. CO. LTD (2019) Code for Design of Retaining Structures of Railway Earthworks. Beijing, China
- Deng B, Yang M (2019) Bearing capacity analysis of pile-stabilized slopes under steady unsaturated flow conditions. *Int J Geomech* 19(12):04019129. [https://doi.org/10.1061/\(ASCE\)GM.1943-5622.0001509](https://doi.org/10.1061/(ASCE)GM.1943-5622.0001509)
- Dong-ping D, Liang L, Lian-heng Z (2017) Limit-equilibrium method for reinforced slope stability and optimum design of antislid micropile parameters. *Int J Geomech* 17(2):06016019. [https://doi.org/10.1061/\(ASCE\)GM.1943-5622.0000722](https://doi.org/10.1061/(ASCE)GM.1943-5622.0000722)
- Dong J (2007) Study on three-dimensional soil arching effect of cantilever piles and ground resisting force acted on its build-in zone. Dissertation, College of civil engineering of Chongqing University
- El Sawwaf MA (2005) Strip footing behavior on pile and sheet pile-stabilized sand slope. *J Geotech Geoenviron Eng* 131(6):705–715. [https://doi.org/10.1061/\(ASCE\)1090-0241\(2005\)131:6\(705\)](https://doi.org/10.1061/(ASCE)1090-0241(2005)131:6(705))
- Ersoy H, Kaya A, Angn Z, Da S (2020) 2D and 3D numerical simulations of a reinforced landslide: a case study in NE Turkey. *J Earth Syst Sci* 129(1):82. <https://doi.org/10.1007/s12040-020-1343-y>
- Gao YF, Ye M, Zhang F (2015) 3-dimensional analysis of slopes reinforced with piles. *J Cent South Univ* 22(6):2322–2327. <https://doi.org/10.1007/s11771-015-2757-6>
- Guo WD (2015) Nonlinear response of horizontally loaded rigid piles in sliding soil. *Can Geotech J* 52(7):903–925. <https://doi.org/10.1139/cgj-2014-0168>
- Hassiotis S, Chameau JL, Gunaratne M (1997) Design method for stabilization of slopes with piles. *J Geotech Geoenviron Eng* 123(4):314–323. [https://doi.org/10.1061/\(ASCE\)1090-0241\(1997\)123:4\(314\)](https://doi.org/10.1061/(ASCE)1090-0241(1997)123:4(314))
- He Y, Hazarika H, Yasufuku N et al (2015) 3-dimensional limit analysis of seismic displacement of slope reinforced with piles. *Soil*

- Dyn Earthq Eng 77:446–452. <https://doi.org/10.1016/j.soildyn.2015.06.015>
- Ito T, Matsui T (1975) Methods to estimate horizontal force acting on stabilizing piles. *Soils Found* 15(4):43–59. https://doi.org/10.3208/sandf1972.15.4_43
- Ito T, Matsui T, Hong WP (1981) Design method for stabilizing piles against landslide—one row of piles. *Soils Found* 21(1):21–37. <https://doi.org/10.3208/sandf1972.21.21>
- Karim MR (2013) Behaviour of piles subjected to passive subsoil movement due to embankment construction—A simplified 3D analysis. *Comput Geotech* 53:1–8. <https://doi.org/10.1016/j.compgeo.2013.04.004>
- Kourkoulis R, Gelagoti F, Anastasopoulos I et al (2011) Slope stabilizing piles and pile-groups: parametric study and design insights. *J Geotech Geoenviron Eng* 137(7):663–677. [https://doi.org/10.1061/\(ASCE\)GT.1943-5606.0000479](https://doi.org/10.1061/(ASCE)GT.1943-5606.0000479)
- Lee CY, Hull TS, Poulos HG (1995) Simplified pile-slope stability analysis. *Comput Geotech* 17(1):1–16. [https://doi.org/10.1016/0266-352X\(95\)91300-S](https://doi.org/10.1016/0266-352X(95)91300-S)
- Li A, Dai F, Liu Y, Du H, Jiang R (2021) Dynamic stability evaluation of underground cavern sidewalls against flexural toppling considering excavation-induced damage. *Tunn Undergr Space Technol* 112:103903
- Li C, Wang X, Tang H (2017) A preliminary study on the location of the stabilizing piles for colluvial landslides with interbedding hard and soft bedrocks. *Eng Geol* 224:15–28. <https://doi.org/10.1016/j.enggeo.2017.04.020>
- Li C, Wu J, Tang H (2016) Model testing of the response of stabilizing piles in landslides with upper hard and lower weak bedrock. *Eng Geol* 204:65–76. <https://doi.org/10.1016/j.enggeo.2016.02.002>
- Lim K, Li AJ, Schmid A et al (2016) Slope-stability assessments using finite-element limit-analysis methods. *Int J Geomech* 17:06016017. [https://doi.org/10.1061/\(ASCE\)GM.1943-5622.0000715](https://doi.org/10.1061/(ASCE)GM.1943-5622.0000715)
- Liu D, Hu X, Zhou C et al (2020) Model test study of a landslide stabilized with piles and evolutionary stage identification based on thermal infrared temperature analysis. *Landslides* 17(6):1393–1404. <https://doi.org/10.1007/s10346-020-01355-0>
- Michalowski RL, Drescher A (2009) 3-dimensional stability of slopes and excavations. *Géotechnique* 59(10):839–850. <https://doi.org/10.1680/geot.8.P.136>
- Onyango JA, Zhang CY (2019) Numerical analysis of slope stability by strength reduction in finite elements using ANSYS a case study of Qinglong–Xingyi expressway contract section T1(K11+790~K11+875). *Environ Earth Sci Res J* 6:89–96. <https://doi.org/10.18280/eesrj.060206>
- Premalatha PV, Kumar SS, Baskar K (2017) Influence of change in pile diameter at various locations of a pile group in a Berthing Structure. *Indian Journal of Geo-Marine Sciences* 46(6): 1198–1209. <http://nopr.niscair.res.in/handle/123456789/41993>. Accessed June 2017
- Rifat Kahyaoglu M, Imancli G, Ugur Ozturk A et al (2009) Computational 3D finite element analyses of model passive piles. *Comput Mater Sci* 46(1):193–202. <https://doi.org/10.1016/j.commatsci.2009.02.022>
- Sharafi H, Sojoudi Y (2016) Experimental and numerical study of pile-stabilized slopes under surface load conditions. *Int J Civ Eng* 14(4B):221–232. <https://doi.org/10.1007/s40999-016-0017-2>
- Won J, You K, Jeong S (2005) Coupled effects in stability analysis of pile–slope systems. *Comput Geotech* 32(4):304–315. <https://doi.org/10.1016/j.compgeo.2005.02.006>
- Xie M, Zheng J, Zhang R (2020) Performance of a combined retaining wall structure supporting a high embankment on a steep slope: case study. *Int J Geomech* 20(6):05020002. [https://doi.org/10.1061/\(ASCE\)GM.1943-5622.0001644](https://doi.org/10.1061/(ASCE)GM.1943-5622.0001644)
- Xu J, Niu F (2014) Safety factor calculation of soil slope reinforced with piles based on Hill’s model theory. *Environ Earth Sci* 71(8):3423–3428. <https://doi.org/10.1007/s12665-013-2730-3>
- Yamin MM (2020) Horizontal response of drilled shafts in a moving cohesive soil. *Int J Civ Eng* 18(7):735–742. <https://doi.org/10.1007/s40999-019-00491-6>
- Yang X-L, Xu J-s (2017) 3-dimensional stability of two-stage slope in inhomogeneous soils. *Int J Geomech* 17(7):06016045. [https://doi.org/10.1061/\(ASCE\)GM.1943-5622.0000867](https://doi.org/10.1061/(ASCE)GM.1943-5622.0000867)
- Yuan S, Du J (2018) Effective stress-based upper bound limit analysis of unsaturated soils using the weak form quadrature element method. *Comput Geotech* 98:172–180. <https://doi.org/10.1016/j.compgeo.2018.02.008>
- Yuan B, Li Z, Su Z, Luo Q, Chen M, Zhao Z (2021) Sensitivity of multistage fill slope based on finite element model. *Adv Civil Eng* 2021:6622936. <https://doi.org/10.1155/2021/6622936>
- Zhang C, Jiang G, Su L (2020) Large-scale shaking table model test on seismic performance of bridge-pile-foundation slope with anti-sliding piles: a case study. *Bull Eng Geol Env* 79(3):1429–1447. <https://doi.org/10.1007/s10064-019-01614-y>
- Zhang G, Wang L (2010) Stability analysis of strain-softening slope reinforced with stabilizing piles. *J Geotech Geoenviron Eng* 136(11):1578–1582. [https://doi.org/10.1061/\(ASCE\)GT.1943-5606.0000368](https://doi.org/10.1061/(ASCE)GT.1943-5606.0000368)
- Zhang SN (2019) Analysis of slope stability and anti-slide pile optimization based on Abaqus. Dissertation, Hebei University of Engineering
- Zhao G, Yang Y, Zhang H et al (2019) A case study integrating field measurements and numerical analysis of high-fill slope stabilized with cast-in-place piles in Yunnan, China. *Eng Geol* 253:160–170. <https://doi.org/10.1016/j.enggeo.2019.03.005>
- Zheng Y, Chen C, Liu T (2020) Analysis of a retrogressive landslide with double sliding surfaces: a case study. *Environ Earth Sci*. <https://doi.org/10.1007/s12665-019-8741-y>

Publisher's Note Springer Nature remains neutral with regard to jurisdictional claims in published maps and institutional affiliations.